Local-density self-consistent energy-band structure of cubic CdS

Alex Zunger* and A. J. Freeman

Department of Physics and Astronomy, and Materials Research Center, Northwestern University, Evanston, Illinois 60201

(Received 9 February 1978)

Self-consistent *ab initio* studies of the electronic-energy-band structure of cubic CdS are reported within the local-density-functional (LDF) formalism. All electrons are included using our previously reported linear-combination-of-atomic-orbitals method in a numerical basis representation. In the first set of calculations we employ the same lattice constant, exchange (only) potential, and computational parameters as were used by Stukel *et al.* in their early self-consistent orthogonalized-plane-wave (SCOPW) investigation so that a direct comparison of results can be made and the validity of the SCOPW approach for covalently bonded 4*d* systems can be assessed. In the second set of calculations, the Stukel *et al.* computational restrictions are relaxed, a more accurate lattice parameter is employed, and the Kohn-Sham exchange and the Singwi *et al.* correlation potential are used to obtain the local-density formalism solutions to the band problem, including variation of the band structure and related properties with pressure (change of lattice constant). Comparison with optical and x-ray and uv photoemission experiments for excitations of both the *s*-*p* and metal *d* bands in the 5–19 eV region indicate very good agreement. The direct gap at Γ is, however, found to be 0.5 eV (25%) too small, a discrepancy similar to that previously found in nonempirical studies for other heteropolar insulators (e.g., Ne and LiF). This is traced to the neglect of the different orbital relaxation at the Γ_{25} and Γ_1 band edges and to the noncancellation of the self-interaction terms characteristic of the local-density potential. Simple atomic total-energy models for these effects are shown to bring this gap into good agreement with experiment. It is concluded that a first-principles (parameter-free) exchange and correlation LDF model describes very well the main electronic-structure features of the system.

I. INTRODUCTION

There now exists vast literature comprising experimental and theoretical investigations of the electronic structure and related properties of the important II-VI compounds. Of obvious importance for understanding and interpreting many of the observed properties of these materials is a detailed knowledge of their underlying electronic band structures. In this regard, recent optical and photoemission experiments have played an important role in elucidating key features of the band structure over an increasingly large range of energies above the fundamental band gap.

On the theoretical side, pioneering *ab initio* energy-band studies[1-5] were carried out for many of these materials using the non-muffin-tin self-consistent orthogonalized-plane-wave (SCOPW) method. This technique has been applied in recent years to the study of the electronic structure of a large number of semiconductors and semimetals, and has resulted in a considerable gain in insight into the systematics of both the III-V and III-VI compounds as well as in a better understanding of the photoemission, high-pressure, and optical data for these materials. At that time, the only popular alternative method was the non-self-consistent empirical pseudopotential approach[6,7] which completely avoided the specification of the microscopic potential in the solid (i.e., the nature of the Coulomb exchange and correlation fields) by pa-

rametrizing empirically the first few Fourier components of an unspecified crystal potential. Although this phenomenological approach has produced a great deal of information on the variation of the gaps in II-VI compounds and the origin of the important band-structure critical points in the Brillouin zone, no meaningful comparison of the adequacy of the SCOPW approach, as well as that of the underlying exchange models, could be made. More-recent developments in semiempirical nonlocal (non-self-consistent) pseudopotential theory[8] have improved considerably the agreement between the calculated band structure and x-ray and uv photoemission data by introducing a few additional disposable parameters to describe the geometry of the angular-momentum-dependent model pseudopotential terms. Although a successful parametrization scheme, little could be learned regarding the microscopic nature of the elementary interactions which lead to this success. Further, due to the independence of the parametrized model potential on its associated variational wave function, questions such as self-consistency and the nature of the crystal dissociation products [which are well-defined local-density-functional (LDF) atoms in both linear-combination-of-atomic-orbitals (LCAO) and SCOPW models] have remained largely unresolved and have inhibited a meaningful comparison with first-principles models based on well-understood (but less successful) crystal potentials. Subsequent studies on the convergence properties

of the orthogonalized-plane-wave (OPW) model,[3,4] independent theoretical studies on compounds made of first-row atoms (diamond,[9] boron nitride[10]) and photoemission studies on the core levels of compounds containing $4d$ elements,[11,12] have revealed serious difficulties with the OPW representation. These include (i) errors of the order of 1–3 eV in the calculated p-like valence- and conduction-band states of compounds made of first-row atoms due to convergence difficulties in the absence of a pseudopotential cancellation for these $l = 1$ states[3,4,9,10]; (ii) spurious shifts of about 12 eV of the corelike $4d$ levels in the course of the self-consistent treatment[5]; and (iii) errors in excess of 6 eV in the level ordering of the cation $4d$ and anion s bands relative to recent photoemission data.[11-14]

This paper presents a self-consistent all-electron first-principles electronic-band-structure study of cubic CdS carried out within the LDF formalism, using our previously developed LCAO technique[15,16] in a numerical-basis-set representation. Long a favorite II-VI compound for study, recent interest in the electronic structure of CdS derives from its use in solar cells[17] (e.g., in CdS-Cu$_2$S heterojuctions) and the observation of electron-hole complexes for high excitation densities in this material.[18,19] Our principal motivation for undertaking this study was to provide an independent rigorous test of the SCOPW method for solving the local-exchange problem[20] for covalent solids. Although the recent advent in first-principles self-consistent LCAO techniques using analytic basis sets [e.g., the linear combination of Gaussian orbitals[21,22] (LCGO)] has permitted an independent test of the predictions of the discrete variational (nonlinearly optimized) numerical-basis-set approach[15,16] for some simple crystals,[9,23] such a comparison with the SCOPW model for transition or fourth-row metal compounds is unavailable at present, primarily due to the practical difficulty in providing sufficient variational flexibility using linear (energy-independent) simple basis sets in the LCGO representation.

For these reasons, as a major part of this work, we present in Sec. II a direct comparison of the results of the SCOPW model with those obtained using the present approach. To ensure a meaningful comparison we keep the same physical content (e.g., lattice parameters, exchange potential) and computational parameters (e.g., number of $\vec{k}$ points used in the Brillouin-zone averages) as were used in the SCOPW model. In Sec. III we apply our method to the same problem, but using this time the full exchange and correlation LDF crystal potential (instead of the exchange-only potential used in the SCOPW work) and the more recently obtained lattice parameters. In addition, we also

vary the relevant computational parameters to convergence. These results permit a discussion of the applicability of the LDF model to the physical properties of the system.

II. SELF-CONSISTENT LCAO EXCHANGE-MODEL STUDIES; COMPARISON WITH THE SCOPW RESULTS

A. Methodology

The method used in these studies has been described previously[15,16] in some detail and so only the essential methodology will be outlined here.

The process by which the LCAO results are obtained starts with the construction of an LCAO-type basis set and the corresponding initial crystal potential. One therefore has to decide which electronic configuration of the constituent atoms is to be used. Since the Cd and S atoms differ in their ionicities (the Pauling electronegativity difference is 0.8), and since there exists a large number of excited atomic states within an energy range characteristic of the band width in CdS, it is not obvious that the neutral-atom ground-state configuration [Cd$(5s^25p^0)$, S$(3s^23p^43d^0)$] form the most appropriate choice. In our scheme[15,16] we generate the basis Bloch orbitals $\Phi_{\mu,\alpha}(\vec{k},\vec{r})$ (for sublattice α and atomic orbital μ) and the crystal superposition potential $V_{\text{sup}}(\rho_{\text{sup}}(\vec{r}))$ from the single-site orbitals $\chi_{\mu\alpha}(\vec{r})$ obtained in a self-consistent solution of the corresponding atomic single-particle equation, assuming the central-field (nl) orbital occupation numbers f_{nl}^α and the net ionic charge Q^α for each atom α. Each such choice $\{f_{nl}^\alpha, Q^\alpha\}$, together with the assumed crystal structure, defined the superposition crystal density $\rho_{\text{sup}}(\vec{r})$ and the corresponding local-density potential $V_{\text{sup}}(\rho_{\text{sup}}(\vec{r}))$ and hence is used to obtain the band structure and the resulting crystal density $\rho_{\text{cry}}(\vec{r})$ (from the band wave functions sampled at a selected set of $\vec{k}$ points in the zone). In the first stage of self-consistency, we minimize iteratively the residual difference $\Delta\rho(\vec{r}) = \rho_{\text{cry}}(\vec{r}) - \rho_{\text{sup}}(\vec{r})$ over the unit cell space, by varying the set $\{f_{nl}^\alpha, Q^\alpha\}$, and select, thereby, the "best" single-site electronic configuration for the superposition representation of the charge density. Note, however, that the nonlinear energy functional entering $V_{\text{sup}}(\rho_{\text{sup}}(\vec{r}))$ (e.g., exchange) are not linearized with respect to the individual single-site densities, as is the case in the first stage of the SCOPW method.[5] Although the establishment of a particular electronic configuration to be used as a starting point in a *fully* self-consistent treatment is theoretically immaterial as long as convergence can be demonstrated, we find that a minimization procedure leading to such an optimal configuration is extremely useful in practice (see below). While one can proceed

directly to find the optimal configuration $\{f_{nl}^{\alpha}, Q^{\alpha}\}$ for Cd and S that minimizes $\Delta\rho(\vec{r})$ in the least-squares sense,[15,16,23] it is instructive to follow this procedure in some detail—as is done in the Appendix—so as to gain some insight into the role of charge transfer and intrasite excitations in this system. This procedure results in an optimal configuration $Cd^{1.05+}(5s^{0.85}5p^{0.10})$ and $S^{1.05-}(3s^{1.95}3p^{4.90}3d^{0.20})$.[24]

Clearly, a superposition representation of the charge density of a covalently bonded material cannot account for the full anisotropy of the charge density[9,10] both due to the inherent spherical site symmetry of the underlying *atomic* densities $\sum_{\mu}|\chi_{\mu\alpha}(\vec{r})|^2$ and due to the restriction of the expansion centers to coincide with the actually occupied atomic sites in the solid. Hence, although $\Delta\rho(\vec{r})$ can be minimized within the superposition model, it cannot, in general, be reduced to zero (or a constant) in a covalently bonded system, even by nonlinear optimization processes. We hence proceed in stage 2 of full self-consistency by treating the *residual* charge density difference, $\tilde{\Delta}\rho(\vec{r})$ (i.e., that resulting from the last iteration of stage 1 in the self-consistency) beyond the superposition representation. This can be done either by using real-space techniques that project $\Delta\rho(\vec{r})$ onto some multicenter basis set (e.g., atom plus bond-centered Gaussians[25]) or by reciprocal-space techniques in which $\tilde{\Delta}\rho(\vec{r})$ is expanded in symmetrized plane waves.[25,26] In both cases (and in the mixed-representation technique[25]), one uses the analytic representation of $\tilde{\Delta}\rho(\vec{r})$ to solve the associated Poisson equation and obtain the correction to the interelectronic Coulomb potential and the modified exchange potential $V_x(\rho_{sup}(\vec{r}) + \Delta\tilde{\rho}(\vec{r}))$ needed to proceed to full self-consistency. We find that in the case of a covalently bonded material such as CdS, the residual density $\Delta\rho(\vec{r})$ tends to delocalize smoothly over large parts of the unit cell volume (e.g., the antibond sites as well as the bond regions) with no obvious localization centers and hence an expansion in terms of symmetrized plane waves is both efficient (only the lowest 18 stars are needed) and accurate. Note that, unlike the methods that employ a plane-wave basis set, for a valence calculation in a solid (e.g., the pseudopotential approach in Ref. 8), we do not face the convergence problems associated with a Fourier expansion of the *total* valence densities, and instead, only the smooth part, $\tilde{\Delta}\rho(\vec{r})$, has to be treated. In this context, a careful selection of the electron configuration $\{f_{nl}^{\alpha}, Q^{\alpha}\}$ becomes of practical importance; stage 1 of self-consistency produces not only a nearly self-consistent (SC) result, but also results in a spatially smooth $\tilde{\Delta}\rho(\vec{r})$ [by absorbing all localized features of $\rho_{cry}(\vec{r})$ into

the superposition density] which is readily amenable to a rapidly convergent Fourier representation.

Figure 1 shows the (symmetrized) residual charge density $\tilde{\Delta}\rho(\vec{r})$ obtained in successive iterations in stage 2 of self-consistency,[27] along the [111] bond direction. Inspection of $\tilde{\Delta}\rho^{(1)}(\vec{r})$ shows that at the first iteration in this stage, charge density is displaced from the Cd region to the bond region, with some preferred polarization towards the S site. In addition, some density is accumulated in the Cd core region (relative to the results of the last iteration in stage 1 of self-consistency) at the expense of the density in the antibond region (not shown in this figure). In subsequent iterations, some charge is deleted from the S site and placed on both the Cd site (correcting for some overshooting in the ionic model) and onto the bond center. In is found that 12–18 symmetrized plane waves are sufficient to yield an accurate (≤ 0.02 eV in the eigenvalues) representation of $\tilde{\Delta}\rho^{(n)}(\vec{r})$, and that six (damped) iterations are typically required to achieve full self-consistency [i.e., $|\tilde{\Delta}\rho^{(n)}(\vec{r}) - \tilde{\Delta}\rho^{(n-1)}(\vec{r})| < 5 \times 10^{-5}$ e/a.u.^{3}].
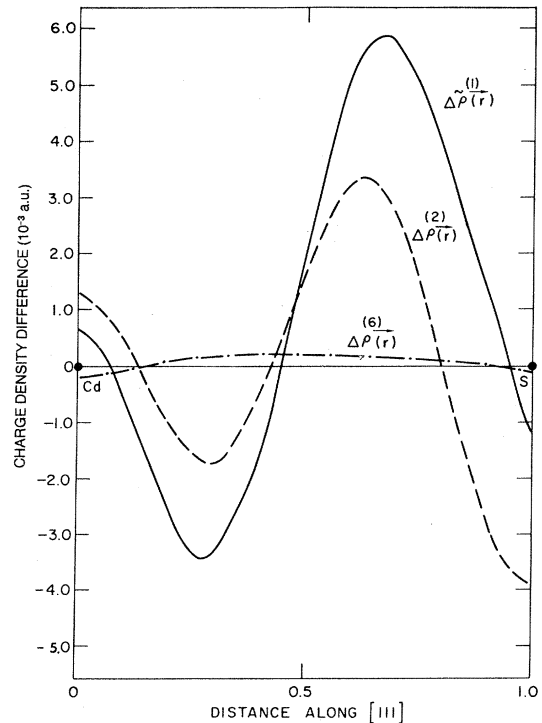
The remaining convergence problems in the

FIG. 1. Variations in the residual densities $\tilde{\Delta}\rho^{(n)}(\vec{r})$ along the [111] bond direction in CdS, for iteration $n = 1$, 2, 6 in step 2 in self-consistency, in the $\alpha = 1$ exchange model.

present technique involve (i) the increase of the direct-space cutoff distance R_c necessary to converge the crystal potential and basis Bloch functions; (ii) the number of Diophantine integration points N_D required for matrix element evaluation[15,16]; and (iii) the number of basis functions. We find that in (i), a use of $R_c = 23$ a.u. produces band eigenvalues that are accurate to within 0.03 eV in the valence bands and 0.07 eV in the conduction bands for energies lower than 8 eV above the valence-band edge. For (ii), we find that a similar accuracy requires about $N_D = 3200-4000$ in the unit cell. For (iii), we find that the inclusion of the Cd $5p$ and S $3d$ is absolutely essential for similar accuracy[28] (e.g., changes of 0.6 eV in the valence bands and up to 1.1 eV in the conduction bands occur if they are omitted) but that inclusion of additional functions (e.g., doubling the number of Cd s and S p orbitals by adding the neutral-atom Cd^0 $5s$ and S^0 $3p$ in addition to the optimized $Cd^{Q+}S^{Q-}$ orbitals) results in much smaller differences. We find that the addition of a S $4s$ orbital causes its admixture into the bottom of the conduction band ($\Gamma_{1,c}$), but changes the direct band gap ($\Gamma_{15,v}-\Gamma_{1,c}$) by less than 0.05 eV. We conclude that the present approach gives an average accuracy of 0.1 eV or better, in the band eigenvalues, for energies below 8 eV above the valence edge.

B. LCAO results and comparison with SCOPW results

The SCOPW model was applied to cubic CdS,[5] using the nonrelativistic local-exchange crystal potential [i.e., the $\rho^{1/3}$ form with an exchange coefficient $\alpha = 1$ ("Slater exhange"[20])]. This particular choice of exchange model was motivated by the previous experience (mainly with non-self-consistent studies) that indicated that this choice leads to better agreement with the experimentally observed optical band gaps than does the use of the "Kohn and Sham" $\alpha = \frac{2}{3}$ value. Our own choice for self-consistent studies[9,10,15,16,23] has been to avoid such empirical adjustment and to use the variationally correct $\alpha = \frac{2}{3}$ value[29] together with the next higher term in the gradient expansion of the exchange and correlation energy, namely, the homogeneous correlation term, for which we adopted the functional calculated by Singwi et al.[30] In the present section, however, we adopt the same exchange potential choice $\alpha = 1$, neglecting correlation terms in order to keep our model as close as possible to that used in the SCOPW calculations.

The cubic-lattice constant of CdS was estimated by Stukel et al.[5] by assuming that the unit cell volume is exactly half of that of the corresponding wurtzite (hexagonal) modification. Using $a_h = 4.13$ Å and $c_h = 6.69$ Å for the hexagonal phase,[31] they

TABLE I. Comparison of SCOPW and LCAO energy eigenvalues for cubic CdS in the $\alpha = 1$ exchange model, using $a_c = 6.081$ Å. W_{VB} denotes the valence-band width and $\langle Cd, 4d \rangle_\Gamma$ indicates the center of gravity of the Cd $4d$ band at Γ. Results are given in eV relative to the top of the valence band $\Gamma_{15,v}$ ($\epsilon_{\Gamma_{15,v}} = -8.95$ eV in the LCAO model). Also shown are the results of two of the empirically adjusted OPW models of Refs. 5 and 35.

Level	SCOPW (Ref. 5)	Present study	Empirical OPW (Ref. 5)	Empirical OPW (Ref. 35)
$\langle Cd, 4d \rangle_\Gamma$	−16.6	− 9.99	−5.7	○ ○ ○
$\Gamma_{1,v}$	−10.92	−11.46	○ ○ •	• • •
$\Gamma_{15,v}$	0.00	0.00	0.00	0.00
$\Gamma_{1,c}$	2.72	2.62	2.5 [a]	2.5 [a]
$\Gamma_{15,c}$	7.58	7.61	9.8	9.2
$X_{1,v}$	− 9.72	−11.42	• • •	○ • •
$X_{3,v}$	− 3.33	− 2.64	−2.2	−2.1
$X_{5,v}$	− 1.44	− 1.06	−0.6	−0.5
$X_{1,c}$	4.89	5.24	6.0	5.1
$X_{3,c}$	5.68	5.45	7.2	7.6
$L_{1,v}$	−10.00	−11.43	○ • •	• • •
$L_{1,v}$	− 3.62	− 2.75	−2.1	−2.4
$L_{3,v}$	− 0.56	− 0.41	0.1	0.0
$L_{1,c}$	4.30	4.04	5.4	5.3
$L_{3,c}$	8.24	8.36	10.1	9.4
$\Gamma_{15,v}-\Gamma_{1,c}$	2.72	2.62	2.5 [a]	2.5 [a]
$L_{3,v}-L_{1,c}$	4.86	4.45	5.3 [a]	5.3 [a]
$X_{5,v}-X_{1,c}$	6.33	6.30	6.6	5.6
$X_{5,v}-X_{3,c}$	7.12	6.51	7.8	8.1
$\Gamma_{15,v}-\Gamma_{15,c}$	7.58	7.61	9.8	9.2
$L_{3,v}-L_{3,c}$	8.80	8.77	10.0	9.4
W_{VB}	3.62	2.75	2.1	2.4

[a] Results adjusted to coincide with experimental estimates.

obtained $a_c = 6.081$ Å for the cubic phase [instead of $a_c = 2(\frac{1}{4}a_h^2 c_h)^{1/3} = 6.111$ Å]. Whereas the observed value appropriate for the cubic phase is[32] $a_c = 5.82$ Å (see also Refs. 33 and 34 that report $a_c = 5.818$ Å), we use in this section the same value, $a_c = 6.081$ Å, as Stukel et al.[5] For the same reason, we use initially only four high-symmetry $\vec{k}$ points (Γ, X, L, and W) with their corresponding nearest-volume weights (0.1258, 0.1731, 0.3600, and 0.3411, respectively) for generating the crystal density from the band wave functions, as recommended by Stukel et al. All of these restrictions will be relaxed in Sec. III.

Table I summarizes the results of the band eigenvalues at Γ, X, and L obtained by the SCOPW[5] and the present model. Also shown are the results obtained by Herman et al.[35] and Stukel et al.[5] using an empirical refinement of their first-principles results by modifying the values of the core shifts and the low-index Fourier components
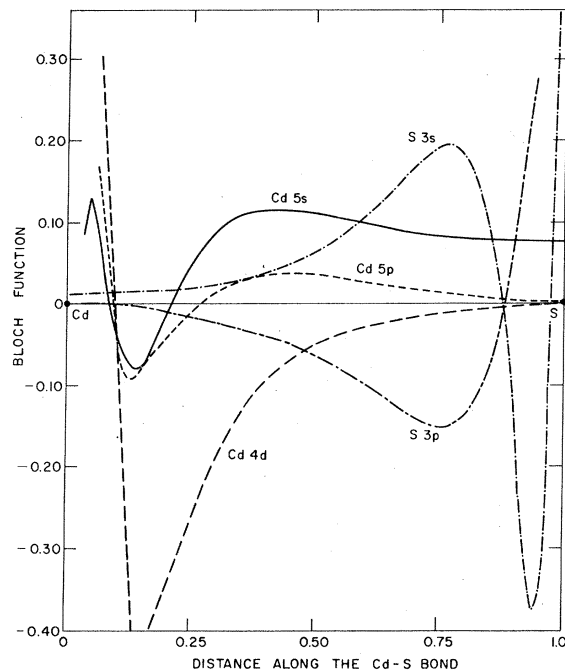
FIG. 2. Charge and configuration self-consistent Bloch basis functions at the Γ point for the CdS system in the exchange and correlation model, along the [111] bond direction in CdS. Some of the radial nodes near the Cd nucleus are omitted.

of the potential. Several conclusions can be drawn from the comparison of the first-principles results:

(i) Excluding the Cd $4d$ band and the lowest sulphur-$3s$-like band ($\Gamma_{1,v}$-$X_{1,v}$-$L_{1,v}$), the average discrepancy for the high-symmetry points shown (for which SCOPW data are available) is 0.52 eV/level in the valence bands and 0.18 eV/level in the conduction bands, although individual differences can be as large as 0.9 eV. Insufficient convergence in the employed basis sets can probably explain only part of this discrepancy; the OPW representation is well converged for states of s and p symmetry around the S site (due to the pseudopotential cancellation associated with the presence of $l = 0, 1$ species in the atomic core) while only states having strong $l = 2$ character around the S site (e.g., $L_{3,c}$, $X_{1,c}$, and $L_{1,c}$) might give rise to convergence difficulties (due to the absence of an S d core). On the LCAO part, the basis set is well converged for the energy range studied (consistent also with the fact that their average discrepancy with the SCOPW results, is higher in the valence bands than in the conduction bands, while basis set shortcomings in the LCAO representations usually reflect themselves in an opposite trend[9,36]).

(ii) The Cd $4d$ band appears in the SCOPW calculations to lie 16.6 eV below the valence-band edge, while in the present study it is at only 10 eV below $\Gamma_{15,v}$. Furthermore, this band shifts by as much as 12.4 eV during the SC iterations in the SCOPW study[5] and lies considerably *below* the S-derived $3s$ band. Empirical adjustments in the SCOPW results,[5] necessary to bring the calculated optical gaps into agreement with experiment, are found to shift the Cd $4d$ band by about 11 eV (placing it above the S $3s$ band). By contrast, we find in our self-consistent model that the Cd $4d$ band lies above the S $3s$ band and shifts only by a small amount (0.8 eV) during iterations.

We note that in the SCOPW model, the Cd $4d$ orbital is treated as a part of the (frozen) core (i.e., the plane waves are explicitly orthogonalized to the atomic Cd $4d$ orbital). Figure 2 shows the Bloch orbitals

$$\Phi_{\mu\alpha}(\vec{k}, \vec{r}) = \sum_n e^{i\vec{k}\cdot\vec{R}_n} \chi_{\mu\alpha}(\vec{r} - \vec{R}_n - \vec{d}_\alpha)$$

(where $\vec{R}_n$ and $\vec{d}_\alpha$ denote unit-cell and inequivalent-site vectors, respectively), for Cd $4d$ and some other representative states. It is clear that the Cd $4d$ state is intermediate between being a core state and a valence state in that it overlaps non-negligibly with other states but still has some localized features. Furthermore, the energy eigenvalue difference between the Cd $4d$ and the S $3s$ in the *free atoms* (2.5 eV)[37] is of a similar order of magnitude to the width of the nearby valence bands in this material,[13,38,39] and d-s hybridization cannot be excluded. Clearly, inclusion of the Cd $4d$ as a *valence* state is hardly practical in the OPW formalism due to the severe plane-wave convergence problems associated with its localized features in real space. Further, considering this orbital as a part of the core is not only in conflict with its valencelike characteristics (cf. also Fig. 9 of the Appendix) and its possible hybridization with the valence states, but would also induce a non-negligible mixing into the OPW's themselves by virtue of its overlap with the valence states ("orthogonality coefficients"). This leads to rather severe convergence difficulties (2–3 eV in valence region for 100–300 OPW's[3]) which are found to be absent in a comparative study on a fictitious Ge crystal[3] having the same structure (but lacking a $4d$ state). It would hence seem that the proper treatment of $4d$ systems in the OPW scheme is an inherent difficulty of the model.

(iii) The lowest-lying S-$3s$-like valence band lies at about 11.4 eV below $\Gamma_{15,v}$ in the LCAO model and is characterized by a low dispersion (~ 0.2 eV), while in the SCOPW model this band lies at 9.7–11

eV below $\Gamma_{15,v}$ and has considerable (1.2-eV) dispersion. This discrepancy is directly attributed to the lack of appropriate Cd $4d$–S $3s$ hybridization in the SCOPW method, due to the reasons discussed in (ii). We find that the S $3s$ band contains some admixture of (σ-type) Cd $4d$ character and that it appears *below* the Cd $4d$ band throughout the zone. The discrepancy in the location of this band between the SCOPW and the present result is 0.5 eV at Γ, 1.7 eV at X, and 1.4 eV at L.

It is interesting to note that the charge transfer between the Cd and S sublattices occurring in the course of the self-consistent treatment tends to diminish the Cd $4d$–S $3s$ gap even to a larger extent than is anticipated from a simple point-ion corrected atomic model (cf., Fig. 9 of the Appendix), facilitating thereby d-s hybridization in the solid. Similarly, the small changes in the radial extension of these orbitals, accompanying charge-transfer effects (cf. Fig. 7 of the Appendix) results in a favorable situation for their mixing (i.e., the orbital moments $\langle r^{-1} \rangle$ are rather similar: 1.1 a.u.$^{-1}$ for Cd $4d$ and 0.85 a.u.$^{-1}$ for S $3s$ at the ionic limit $Q = \pm 1$).

Finally, we have examined the effect of increasing the number of $\vec{k}$ points used to sample the crystal density $\rho_{cry}(\vec{r})$. Comparing our results for four points with that obtained with six points (Γ, X, L, W, Δ, and Σ) we find that the changes in the *relative* location of the bands do not exceed 0.15 eV, while the *absolute* position relative to the vacuum changes by 0.60 eV. We have repeated the calculation for the Γ point using 10 $\vec{k}$ points for the BZ sampling (adding the points K, Σ as well as those halfway between Δ and Γ and L and Γ). This resulted in relative changes of a similar magnitude. The average discrepancies between the present results and the SCOPW results remained roughly unchanged (i.e., increased by about 8%) upon increasing the number of BZ sampling points.

We conclude that the SCOPW model introduces errors of the order of 0.5–1.0 eV in the valence and conduction bands and about a few eV in the lower Cd $4d$ and S $3s$ bands.

III. RESULTS OF THE SELF-CONSISTENT EXCHANGE AND CORRELATION MODEL

A fully self-consistent band calculation was repeated using, this time, the observed lattice constant $a_c = 5.818$ Å,[32-34] and the Kohn and Sham exchange[29] and correlation[30] potential. We have used six $\vec{k}$ points for the BZ sampling, while the other convergence parameters were identical to those used in Sec. II which yield an overall accuracy in the band eigenvalues of 0.1 eV, or better. Figure 3 shows the various components of the
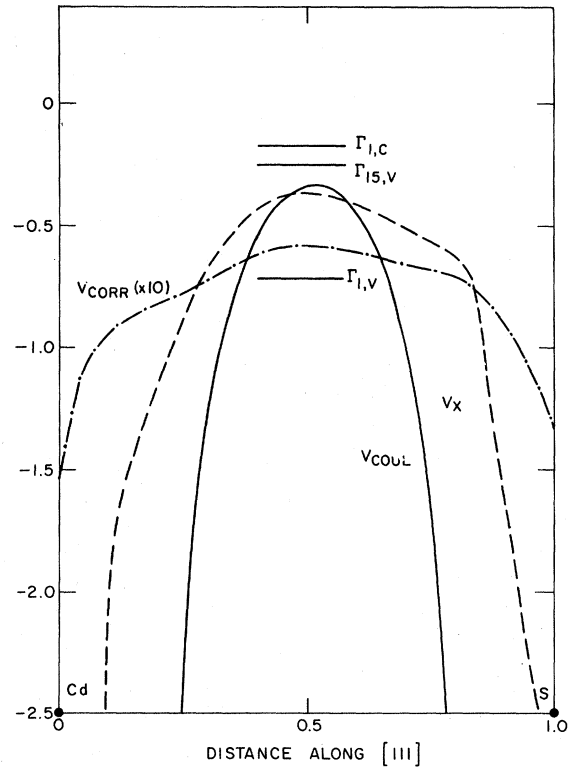

FIG. 3. Components of the self-consistent crystal potential of CdS in the exchange and correlation model, along the [111] bond direction, V_x, V_{corr}, and V_{Coul} denote, respectively, the exchange, correlation, and total coulomb potentials. Also shown are the positions of the lower S-derived $3s$ band ($\Gamma_{1,v}$) and the valence ($\Gamma_{15,\,v}$) and conduction ($\Gamma_{1,\,c}$) band edges, relative to the vacuum.

self-consistent crystal potential along the [111] bond direction. We also indicate, on the same scale, the positions of the bottom of the S $3s$ band ($\Gamma_{1,v}$) as well as the edges of the valence and conduction bands ($\Gamma_{15,v}$ and $\Gamma_{1,c}$, respectively), relative to the vacuum. It is seen that the Coulomb (short-range plus long-range) potential has a similar magnitude as the exchange potential at the bond center, the latter being substantially more asymmetric indicating significant charge polarization along the bond. The correlation potential is smaller by about an order of magnitude than the exchange potential and has a distinctly different spatial form. The resulting band structure is shown in Fig. 4.

Some energy eigenvalues at high-symmetry points are shown in Table II. The density of states, calculated by the analytic tetrahedron method[40] is depicted in Fig. 5. The band structure is characterized by three distinct valence components and a broad conduction band. Between 11 and 12 eV below the upper valence-band edge
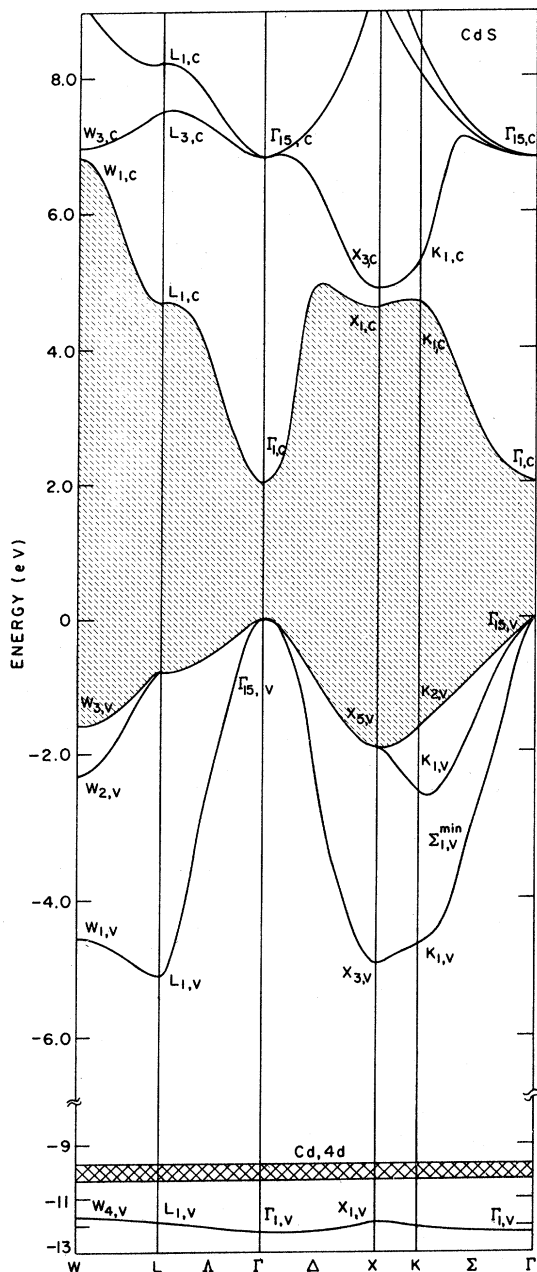
FIG. 4. Self-consistent band structure of cubic CdS in the exchange and correlation model. Note change in scale of the lower part of the figure.

TABLE II. Energy eigenvalues obtained in the SC exchange and correlation model for cubic CdS. Lattice constant $a_c = 5.818$ Å. Energies are given in eV relative to the $\Gamma_{15,v}$ point (located at -6.80 eV).

Level	Energy	Level	Energy
$\Gamma_{1,v}$	-12.27	$L_{1,v}$	-11.92
$\langle \text{Cd}, 4d \rangle_\Gamma$	-9.90	$L_{1,v}$	-5.11
$\Gamma_{15,v}$	0.0	$L_{3,v}$	-0.79
$\Gamma_{1,c}$	2.01	$L_{1,c}$	4.70
$\Gamma_{15,c}$	6.82	$L_{3,c}$	7.52
X_{1v}	-11.82	W_{4v}	-11.70
X_{3v}	-4.92	W_{1v}	-4.52
X_{5v}	-1.90	W_{2v}	-2.30
X_{1c}	4.61	$W_{3,v}$	-1.63
X_{3c}	4.90	W_{1c}	6.82
		W_{3c}	6.95

at Γ, $\Gamma_{15,v}$-$\Gamma_{1,c}$, is 2.01 eV and separates the valence band from the broad conduction band made up of Cd $5s$, $5p$ and S $3d$, $4s$ orbitals.

X-ray-photoemission studies on CdS have been confined to the hexagonal phase. Kindig and Spicer[13] reported results obtained with uv photons in the 6–21-eV range while Ley et al.[11] obtained results with the Al $K\alpha$ radiation (1486 eV), and Sagawa et al.[41] used synchrotron radiation. Using the spectral assignment of Ley et al. for cubic semiconductors, and applying Birman's[42] correlation between the states of the hexagonal and cubic phase, one can compare the observed structure in the valence band with the calculated results (Table III). The agreement appears to be satisfactory (differences are smaller than those usually obtained between ultraviolet-photoemission data[12] and x-ray-photoemission data[11]), and is in line with the findings of Cardona et al.[43] which suggest that the differences in reflectivity between the hexagonal and cubic forms are within 0.1–0.2 eV.

The photoelectron spectra obtained by Sagawa

($\Gamma_{15,v}$) we have a S-3s-derived band having some admixture of σ-type Cd-4d character. At about 2 eV higher in energy we find the Cd-4d-derived band that is about 0.9 eV wide. This band is separated by a wide gap (6.92 eV at X and 6.81 eV at L) from the main valence band that is 5.1 eV wide and is made up of S $3p$ and Cd $5s$ orbitals with slight admixture of S $3d$ and Cd $5p$. The direct gap
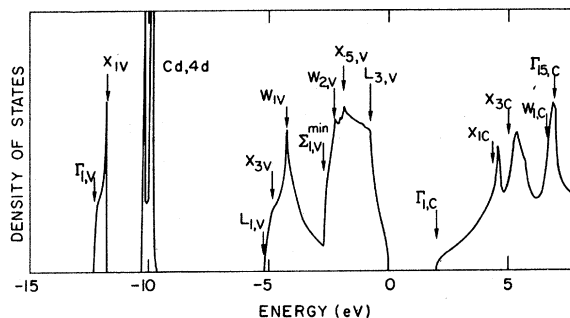

FIG. 5. Density of states of cubic CdS in the self-consistent exchange and correlation model.

TABLE III. X-ray photoemission results (Ref. 11) for the positions of valence-band states, compared with the calculated results. The observed results pertain to the hexagonal phase, and were correlated with the corresponding states in the cubic phase. Results are given in eV relative to the valence edge at $\Gamma_{15,v}$.

Level	Expt.	Calc.
$L_{3,v}$	-0.8	-0.79
$X_{5,v}$	-1.9	-1.90
$W_{2,v}$	-2.2	-2.30
$Z_{2,v}^{min}$	-3.1	-2.62
$W_{1,v}$	-4.3	-4.52
$X_{3,v}$	-4.8	-4.90
$L_{1,v}$	-4.8	-5.11

TABLE V. Comparison of reflectivity peaks (Ref. 43) with the calculated transition energies (in eV) at high-symmetry points. The symbols in column 1 are the standard spectroscopic labels used by Cardona et al. (Ref. 43).

Transition	Expt.	Assignment	Calc.
E_0	2.55	$\Gamma_{15,v} \to \Gamma_{1,c}$	2.01
E_1	5.30	$L_{3v} \to L_{1c}$	5.49
E_0'	6.40	$\Gamma_{15,v} \to \Gamma_{15,c}$	6.82
E_2	7.5	$X_{5v} \to X_{1c}$	6.50
		$X_{5v} \to X_{3c}$	6.80
		$\Sigma_4 \to \Sigma_1$	7.21
E_1'	8.8	$L_{3v} \to L_{3c}$	8.32
d_2	14.4 eV	Cd $4d$–L_{1c}, X_{1c}	14.6, 14.5
$\circ\circ\circ$	16.1, 17.4	S $3s$–$L_{1c}, \Gamma_{15,c}$	16.4, 18.6

et al.[41] show valence-band maxima at 3.4 and 6.0 eV below the valence edge. These should correspond to the first two peaks in the density of valence states (Fig. 5) at ~2 eV (X_{5v}-W_{2v}) and 4.5–4.8 eV (W_{1v}-X_{3v}). These peaks appear in the work of Ley et al.[11] at 1.9–2.3 and 4.5–4.9 eV, in better agreement with our results. We note that the spectral shape and peak positions in the work of Sagawa et al.[41] still shift considerably with changing the photon energy (between 40 and 60 eV), suggesting probable Auger-emission tails or final-state effects.[12]

The location of the singular points in the conduction bands can be deduced from the $L_{II,III}$ absorption studies.[38,39,44] Table IV compares the results using Sugiura's assignment for the L_{II} and L_{III} transitions. The agreement is seen to be very good for the states above 5 eV; however, the discrepancy for the lowest excited state of s symmetry at L is large (17%) and results in an inversion of the order of the L_{1c} and X_{1c} states.

The positions of the reflectivity peaks in cubic CdS (see Ref. 43) are compared in Table V with

TABLE IV. $L_{II,III}$ absorption-spectra results (Ref. 38) for high-symmetry states in cubic CdS. Experimental data include the estimates from the L_{II} and L_{III} spectra. Results in eV relative to the valence-band edge, using the observed optical gap of 2.55 eV (Ref. 43).

Level	Expt.	Calc.
$L_{1,c}$	4.05	4.70
X_{1c}	4.65	4.60
X_{3c}	5.05–5.25	4.90
W_{1c}	6.25–6.65	6.82
L_{3c}	7.65–7.85	7.52

our calculated results, using the "standard" assignment for the spectra of II-VI compounds.[43] Our calculation significantly underestimates the direct $\Gamma_{15,v} \to \Gamma_{1,c}$ band gap, but otherwise yields reasonable results. The spectrum below 9 eV consists of a series of transitions coupling the highest valence band with the conduction bands. At higher energies, a window is observed at 12.5 eV,[43,45] followed by three peaks at 14.4 eV,[43,45] and 16.1 and 17.4 eV.[45] To understand the nature of the broad structure at 12–20 eV, we first determine the positions of the lower valence bands. The x-ray-photoemission data of Ley et al.[11] on hexagonal CdS place the Cd $4d$ band at 9.64 ± 0.09 below the valence-band edge at $\Gamma_{15,v}$. Using the optical value for the band gap, $E_g = 2.55$ eV,[43] one obtains the value of 12.2 ± 0.09 eV for the position of this band relative to the bottom of the conduction band. Using the alternative value of 10.1 eV obtained by Vesely and Langer[14] for the Cd $4d$–$\Gamma_{15,v}$ separation (based on a somewhat uncertain position of the emission line relative to the Fermi energy), the Cd $4d$–Γ_{1c} gap appears to be at 12.65 eV. Our calculated value for the Cd $4d$–Γ_{1c} separation is 11.91 eV. One would hence expect that the absorption spectra above ~12.4 eV to be due to Cd $4d$ to conduction-band transitions. Indeed, examination of the reflectivity data of Cardona et al.[43] and Walker and Osantowski[45] shows an optical window at ~12.5 eV followed by a broad band, which we assign to these transitions. Since the bottom of the conduction band at Γ_{1c} is predominantly of Cd-5s character and hence dipole-forbidden from Cd-4d transitions, one expects to find the maximum of this absorption band around the position of maximum density of states of Cd-5p character in the conduction band. Such states are

found near the $L_{1,c}$ and $X_{1,c}$ levels (Fig. 5) which are located at 2.7 and 2.6 eV, respectively, above the bottom of the conduction band (i.e., 14.6 and 14.5 eV above the center of gravity of the Cd $4d$ band). This corresponds to the observed peaks at 14.4–14.2 eV in the results of Cardona et al.[43] and Walker and Osantowski.[45] The Kramers-Kronig analysis of the reflectivity data of Cardona et al.[43] indicates a local minimum in ϵ_1 and ϵ_2 below the threshold of the Cd-$4d$ to conduction-band transitions. Structure in this region can be attributed to excitonic transitions due to the Cd $4d$ band with a series limit at the bottom of the conduction band at ~12.2 eV. The observed shoulder at 11.9 eV (the d_1 shoulder)[43] might be a plausible candidate for such a transition, corresponding to an exciton binding energy of ~0.3 eV.

About 2 eV below the Cd $4d$ band, we find the S $3s$ band that is expected to give rise to optical transitions to high density-of-states levels of sulphur character in the conduction band (e.g., $\Gamma_{15,c}$) at 16–18 eV. These transitions probably correspond to the observed peaks[45] at 16.1 and 17.4 eV.

Although the agreement between the calculated and observed interband transitions from the semicore states is reasonable, their identification in terms of LDF band eigenvalue differences possess some theoretical problems.[23] One realizes that an *eigenvalue* difference $\Delta\epsilon_{ij}$ between conduction and valence bands forms an adequate approximation to the *total energy* difference ΔE_{ij} (corresponding to the system in the excited and the ground state, respectively) only in the limit where the corresponding electron states are truly delocalized.[46] If some spatial localization is present (e.g., for initial core and semicore states), the difference $\Delta E_{ij} - \Delta\epsilon_{ij}$ is nonzero (usually positive in LDF[23] but negative in the Hartree-Fock model[47]) due to both the spatial relaxation of the corresponding band eigenfunction and the cancellation of the self-interaction terms. It has been previously shown[23] that these effects might (i) cause the breakdown of the LDF *band* model (which identifies excitation energies with band eigenvalue differences) even for the description of valence-to-conduction transitions in ionic materials and possibly in rare-gas solids which are characterized by rather localized orbitals, and (ii) explain in part the reason why the LDF model usual predicts too small excitation energies. Clearly, the relaxation and self-interaction cancellation effects are rather large in atoms, but usually decrease as one goes to molecules, clusters and finally to extended solids. One can hence obtain as estimate for the *upper bound* for these $\Delta E_{ij} - \Delta\epsilon_{ij}$ corrections in the Cd-$4d$ and S-$3s$ spectra by calculating these quantities for the free atoms. One finds that for an *ionization* of

a Cd $4d$ electron in the atom, $\Delta E = 17.65$ eV (using the same exchange-correlation functionals as used for the band study), compared with the observed value of 18.15 eV,[48] while the negative of the Cd $4d$ eigenvalue is $\Delta\epsilon = 11.47$ eV. This leaves a net correction of 6.18 eV for the Cd $4d$ ionization. Similarly, ΔE for ionizing a $3s$ electron in S is 21.23 eV and $\Delta E - \Delta\epsilon = 5.3$ eV for this process. The net estimate for the relaxation and self-interaction correction to the relative Cd-$4d$ and S-$3s$ onsets is hence 0.88 eV. Clearly, this value is rather large relative to the pertinent excitation energies in the crystal and only a full total energy difference calculation in the *solid* (in which the excited species are treated as impurities) such as that reported in Ref. 23 for LiF, can elucidate the role of the relaxation and self-interaction cancellation for these semicore states. In the absence of such a calculation, we can only draw qualitative conclusions: (i) The fact that the band model seems to work well for these excitation processes might indicate that, after all, the Cd $4d$ and S $3s$ band can be described as itinerant states, in which case the relaxation and self-interaction cancellation corrections are a "$1/N$" effect, being distributed over the N particles spanning the corresponding bands. (ii) The fact that the $\Delta E - \Delta\epsilon$ correction is about 1 eV larger for Cd $4d$ than for S $3s$ may result in a situation where the corresponding excitations to the conduction band are even closer in energy than anticipated from the band model (~2 eV difference), leading to a stronger degeneracy of the Cd-$4d$ and S-$3s$ spectra. Note that in turn these spectra are degenerate with the high-energy valence-to-conduction transitions, such as $L_{1,v} \rightarrow L_{1,c}^*$.[49-51] (iii) The $\Delta E - \Delta\epsilon$ correction in atoms decreases for outer-shell excitations relative to inner-shell excitations (e.g., ΔE for ionizing a Cd $5s$ electron is 8.02 eV, compared with the spectroscopically observed value of 8.99 eV,[48] and $\Delta E - \Delta\epsilon$ is 3.4 eV; for the ionization of a S $3p$ electron, the correction is smaller than 2 eV) but are non-negligible even for the valence states. This might result in a situation where even the calculated valence to conduction gap (2.01 eV) would be affected by such corrections. An estimate to that correction can be made by assuming that the valence-band edge is a pure S $3p$ state (in practice it is 91% S $3p$) and the conduction edge is a pure Cd $5s$ state (in practice it is 73% Cd $5s$) and calculating $\Delta E - \Delta\epsilon$ for an S-$3p$ ionization and a Cd-$5s$ electron-capture process in the corresponding *atoms* and *ions* (since the ionicity in the crystal is intermediate between these limits). Such a calculation yields a *net* correction of 1.2 eV for the neutral species Cd^0 and S^0, and 0.9 eV for the Cd^{1+} and S^{1-} species. When applied to the
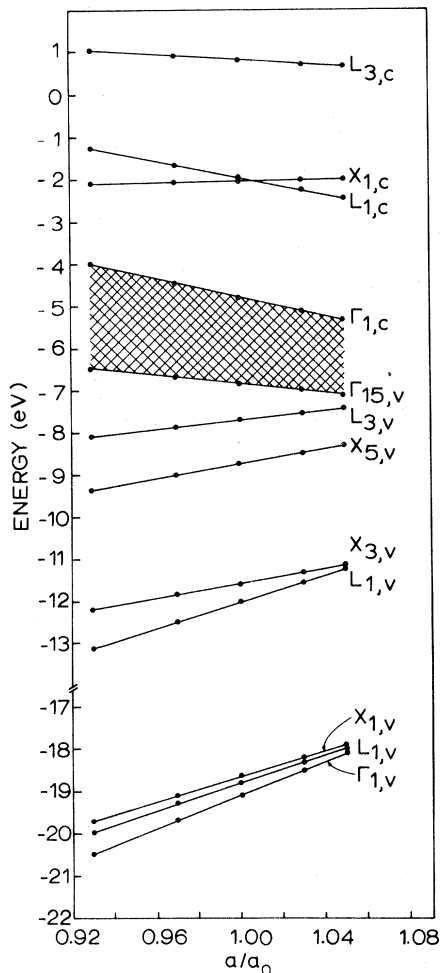
FIG. 6. Variation in some band energies for high-symmetry points in the zone with the reduced lattice constant a/a_0, where $a_0 = 5.818$ Å. The shaded area indicates the direct gap at Γ.

calculated $\Gamma_{15,v}$-$\Gamma_{1,c}$ band gap, this would yield a corrected value of 2.9–3.2 eV, compared with the observed value of 2.55 eV.[43] One might expect that a direct total energy difference calculation for the corresponding transition in the *solid* would yield results that are intermediate between the band-structure prediction (2.01 eV) that assumes complete delocalization of the corresponding band states and the results based on the atomic estimates (2.9–3.2 eV) which assumes localized states. One may further expect that these corrections would be substantially smaller for excitations into higher conduction band states, which are more "free-electron-like," and hence a band model would form a reasonable approximation for these transitions (cf. Table V).

It is possible to compare the absolute positions of our calculated valence- and conduction-band edges, relative to the vacuum level, with the available experimental data. These quantities form a sensitive test of both the accuracy of the self-consistency and of the proper calculation of the Ewald summations in the problem. Swank[52] measured the photoemission yield and the contact potential for CdS crystals. From his results one can obtain the position of the valence- and conduction-band edges in the bulk crystal relative to the vacuum by using the observed values of the band bending, work function at the surface, and Fermi level.[52] This yields $I_{CB} = -4.86$ eV and $I_{VB} = -7.41$ eV for the conduction- and valence-band edges, respectively, which should be compared with our calculated values of -4.79 and -6.80 eV, respectively. The value of the electron affinity I_{CB} obtained by Kindig and Spicer in the high-vacuum photoemission experiment,[13] 4.8 ± 0.3 eV, is likewise similar to our calculated value.

We have also calculated the variation in the band structure with a change in lattice constant. Figure 6 shows the dependence of some high-symmetry band energies with the reduced lattice constant a/a_0, where a_0 is the equilibrium zero-pressure cubic-lattice parameter.

The lower (bonding) S-3s-derived valence-band states at $\Gamma_{1,v}$, $L_{1,v}$, and $X_{1,v}$ are stabilized by reducing the lattice constant and approach a common limit as the crystal is dilated. Similar behavior characterizes the lowest $(X_{3,v}, L_{1,v})$ and upper $(X_{5,v}, L_{3,v})$ parts of the main valence band. The direct $\Gamma_{15,v}$-$\Gamma_{1,c}$ band gap increases with reduction of the lattice constant. In analogy with Ge, where it was found that most of the characteristic changes in the optical spectra in going from an ordered to an amorphous solid can be rationalized in terms of a band model for an ordered crystal but with an increased lattice parameter (corresponding to the dilated amorphous state[53]), our findings suggests that amorphous CdS would have a substantially smaller gap than does the ordered material. A dilation of $a/a_0 \approx 1.05$ is expected to shift the band gap to approximately the center of the solar spectrum, making CdS a more efficient absorber in solar cell devices. We similarly find that the prominent structure in the absorption spectra, e.g., the E_1 peak $(L_{3v}$-$L_{1c})$, the E_2 peak $(X_{5v}$-$X_{1c})$ and the E_1' peak $(L_{3v}$-$L_{3c})$ increases almost linearly when the crystal is compressed, in agreement with experimental findings for some other II-VI compounds.[54]

It is interesting to note that the lowest conduction state at X changes only slightly with variation of a in the region $0.95 \lesssim a/a_0 \lesssim 1.05$, similar to the situation found by us for boron nitride.[10] Hence, our calculation predicts that while the direct $\Gamma_{15,v}$-$\Gamma_{1,c}$ gap increases with pressure, the indirect

$\Gamma_{15,v}$-$X_{1,c}$ gap decreases with pressure. There is no experimental evidence to test this result as yet, but pressure experiments on gallium arsenide[54–56] (which also has a conduction-band minimum at Γ and a secondary minimum around X) have indicated a positive pressure coefficient for the lowest transition at Γ, with a negative coefficient for the higher set of minima. Clearly, experiments of this kind for CdS would help to assess the validity of our model.

Another point worth mentioning is the crossing of the conduction-band minima at X and L with variation in a/a_0; while the X_{1c} point is above the L_{1c} point for $a/a_0 \geq 1.05$, the order is reversed for smaller lattice parameters. The width of the main valence band is shown to decrease with dilation and similarly the splitting of the conduction bands, X_{1c}-X_{3c}, is lowered from 0.70 to 0.20 eV upon changing a/a_0 from 0.95 to 1.05.

Finally, we need to discuss the possible importance of relativistic corrections which have been completely ignored in this work. Rough estimates of these effects may be obtained by use of atomic models. We have solved the Dirac-Slater (relativistic) equations for a free Cd atom and compared the results with solutions of the Hartree-Fock-Slater (nonrelativistic) equations using, in both cases, $\alpha = \frac{2}{3}$ for the coefficient of exchange. The Cd 5s level is found to be lowered in energy by 0.39 eV (due to the usual effect of the mass-velocity and Darwin terms) whereas the Cd 4d eigenvalue *increases* by 0.44 eV (for $j = \frac{3}{2}$) and 1.14 eV (for $j = \frac{5}{2}$) (due to greater screening of the nucleus caused by contraction in space of the s electrons). Since the S energy levels are not expected to be changed by relativistic effects, the net effect is to *increase* the gap between the S 3s and Cd 4d bands in the solid. Further, since the conduction band minima in CdS comes from a Cd-5s-based state, one would hence expect the band gap to be *reduced* by 0.4 eV in the relativistic case. The nonrelativistic band gap, as obtained in this work is 2 eV while self-interaction and relaxation corrections, applied to this nonrelativistic gap yield $E_g \approx 2.9$–3.2 eV. Thus, one would expect that a relativistic local exchange band gap would be of the order of 2.5–2.8 eV, in reasonable agreement with experiment ($E_g = 2.55$ eV). Thus, due to the partial cancellation between relativistic effects on the one hand (reducing E_g) and relaxation self-interaction effects on the other hand (increasing E_g) it has been possible to obtain a reasonable description of the spectrum simply by introducing small adjustments into the potential parameters of a nonrelativistic local-density band structure.[5] A more fundamental approach that recognizes the inherent state dependence of both the local-density

quasiparticle excitation spectra and relativistic effects, would systematically correct the eigenvalue spectrum by using models for the relaxation and self-interaction effects and relativistic effects.[57,58]

APPENDIX : PROCEDURE FOR DETERMINING THE OPTIMAL VALUES OF THE INITIAL LCAO BASIS SET AND CRYSTAL POTENTIAL

Consider, for example, the partially ionic system $Cd^Q{}^+S^{Q-}$ with the particular charge transfer pattern in which Cd s electrons are transferred to the unoccupied S p shell: $Cd^Q(5s^{2-Q}5p^0)$ and $S^{Q-}(3s^23p^{4+Q}3d^0)$. We first consider the effect of this charge transfer on the basis orbitals $\chi_{\mu\alpha}(\vec{r})$. Figure 7 shows the calculated moments $\langle r^{-1}\rangle_{\mu\alpha}$ and $\langle r^{-3}\rangle_{\mu\alpha}$ for $\alpha\mu =$ Cd 4d, Cd 5s, and Cd 5p as well as S 3s, S 3p, and S 3d as a function of the assumed ionicity Q. It is evident that the Cd orbitals contract while the S orbitals expand radially as Q increases between 0 and 2, the effect being less pronounced in the localized orbitals (Cd 4d, S 3s) than in the diffuse orbitals. Figure 8 shows the differ-
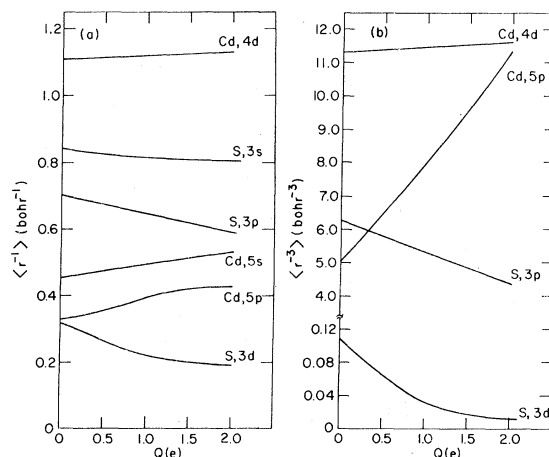

FIG. 7. Dependence of the first (a) and the third (b) negative orbital moments of Cd and S ions, on the fractional ionic charges in the $Cd^{Q+}(5s^{2-Q}5p^0)S^{Q-}(3s^23p^{4+Q}3d^0)$ configuration.
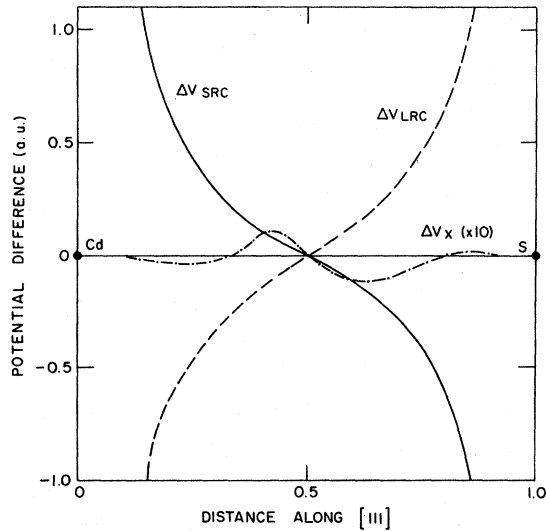
FIG. 8. Difference in the short-range Coulomb (SRC), long-range Coulomb (LRC), and exchange (x) potentials of the $Q = \pm 1$ ionic model and the neutral model for cubic CdS, plotted along the [111] bond distance.

ence $\Delta V(\vec{r})$ between the components of the ionic $(Q=1)$ superposition potential and the neutral potential $(Q=0)$, along the bond [111] crystal direction. We have indicated separately the difference in the crystal short-range Coulomb field $\Delta V_{SRC}(\vec{r})$ [i.e., that due to the electron-electron Coulomb potential, plus the electron-screened nucleus $(Z_{eff}=Z-Q)$ potential], the long-range Coulomb field $\Delta V_{LRC}(\vec{r})$ (due to the Madelung-type point-ion interactions) and the exchange potential $\Delta V_x(\vec{r})$. It is seen that due to the contraction of the Cd orbitals in the ionic case, the exchange field is more attractive near the Cd site in this model and conversely, the more diffused S orbitals lead to a less attractive exchange potential near the S site in the ionic models. The ionic potential has a more repulsive short-range Coulomb potential near the Cd site, but possesses an additional long-range Madelung field which is absent in the neutral limit. The net Coulomb effect is to produce a more attractive field in the Cd region and a more repulsive field in the S region (similar to the effects in the exchange potential). It is hence clear that by varying the ionicities in this system one introduces an additional *asymmetry* in the potential (relative to the neutral potential) and that one cannot expect to obtain just a rigid shift in the resulting band structure, since the crystal symmetry permits the formation of band states that weight preferably orbital contributions from a single sublattice.

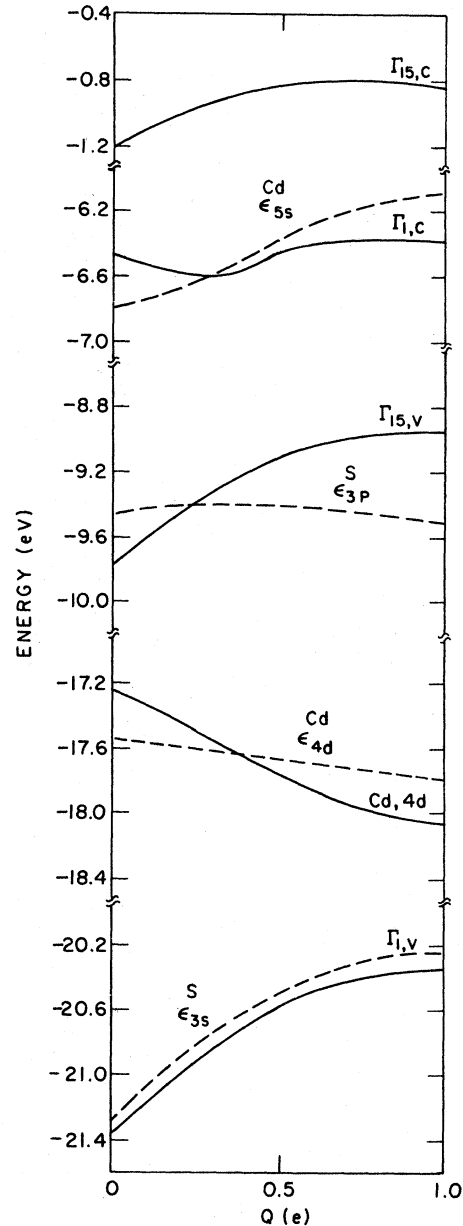Figure 9 shows the change in the band eigenvalues for some high-symmetry states in the crystal

FIG. 9. Variation of some band energies at high-symmetry points in the zone with the assumed ionicity, in the non-SC $\alpha = 1$ exchange model for cubic CdS. The dashed lines indicate the variation in the corresponding free-ion eigenvalues, corrected for the point-ion field at the ionic site: $\epsilon_\mu^\alpha = \epsilon_\mu^\alpha + QV_M$, where the Madelung field is $V_M = 8.95$ eV for this model.

(full lines), as a function of the ionicity Q assumed in generating both the Bloch basis functions and the potential. It is seen that crystal states that are formed predominantly from S orbitals (e.g., the bottom of the lowest valence band at $\Gamma_{1,v}$ or the top of the highest valence band at $\Gamma_{15,v}$) are de-

stabilized by increasing the ionicity, while states formed predominantly from the Cd sublattice orbitals (e.g., the Cd $4d$ band) are stabilized by the ionicity. Crystal states that are extended over large portions of the unit cell space covering both sublattices (e.g., the conduction states $\Gamma_{1,c}$ and $\Gamma_{15,c}$) vary much less with ionicity due to the partial cancellation of the effects introduced by the positive and negative lattice sites. We have also shown in Fig. 9 the variation in the atomic eigenvalues $\epsilon_{\mu\alpha}$ corrected by the Madelung field at the corresponding ionic sites ($\bar{\epsilon}_{\mu\alpha} = \epsilon_{\mu\alpha} + QV_M$, where V_M is calculated to be 8.95 eV for the face-centered-cubic lattice with $a_c = 6.081$ Å). It is seen that the point-ion corrected eigenvalues follow the general trends in the corresponding band states, the remaining differences being due to band-structure effects (e.g., orthogonality of the band states, intersite overlap, and exchange nonlinearity). It is particularly interesting to note in this context that the Cd-$4d$ point-ion-corrected atomic eigenvalue deviates significantly from the corresponding band energy. This stems directly from the noncore character of this orbital which makes it susceptible to band structure effects. A second point worth noting is that the variation of the upper valence- and conduction-band eigenvalues with ionicity is rather weak in the $Q \gtrsim 0.8e$ region (resulting, for instance, in relatively small changes in the direct $\Gamma_{15,v}$-$\Gamma_{1,c}$ band gap in this region). It is found that in this region of ionicities, the increased repulsion in the short-range Coulomb potential $V_{\mathrm{SRC}}(\vec{r})$ in the Cd region, is almost exactly balanced by the combined effect of the increased

attractiveness of the long-range Coulomb and the exchange potentials $V_{\mathrm{LRC}}(\vec{r}) + V_x(\vec{r})$ [i.e., $\Delta V_{\mathrm{SRC}}(\vec{r}) + \Delta V_{\mathrm{LRC}}(\vec{r}) + \Delta V_x(\vec{r})$ is approximately position independent].

Interestingly, a direct minimization of $\Delta\rho(\vec{r})$ as a function of $\{f_{nl}^\alpha, Q^\alpha\}$ yields an optimal value of $Q_{\mathrm{Cd}} = -Q_{\mathrm{S}} = 1.05e$, which occurs in this region of stability. Of course, since such a minimization procedure involves more than the transfer of Cd $5s$ charge to the S $3p$ orbital, which we have assumed for illustrative purposes only, additional modes are possible. To keep the number of the charge deviation minimization parameters tractable, we have allowed only four degrees of freedom, namely, the Cd configuration ($\cdots 4d^{10}5s^{2-Q_1}5p^{Q_2}$) and S($\cdots 3s^{2+Q_3}3p^{4+Q_4}3d^{Q_5}$), where the Cd charge $Q = Q_1 - Q_2$ equals the negative of the S charge, $-(Q_3 + Q_4 + Q_5)$, by the requirement of charge neutrality. (We have hence assumed that the *population* of the closed shell ions Cd^{2+} and S^{6+} do not change in the crystal, but that their eigenvalues and orbitals can change in response to charge redistribution in the valence manifolds.) The resulting optimal configuration $\mathrm{Cd}^{1.05+}(5s^{0.85}5p^{0.10})$ and $\mathrm{S}^{1.05-}(3s^{1.95}3p^{4.90}3d^{0.20})$ indicates that indeed the Cd $5s \to$ S $3p$ promotion is the leading charge transfer in the system, and that additionally, a non-negligible population of the formerly virtual atomic orbitals (Cd $5p$, S $3d$) occurs (this allows for a more efficient variational participation of these plane-wave-like orbitals into the band states, as indicated by a corresponding increase in the resulting LCAO expansion coefficients).

---

*Present address: Dept. of Physics, University of California, Berkeley, Calif. 94720.

[1] F. Herman, R. L. Kortum, I. B. Ortenburger, and J. P. Van Dyke, Electronic Structure and Optical Spectrum of Semiconductors, Aerospace Report 69-0080, Wright-Patterson Air Force Base, Ohio, 1969 (unpublished).

[2] R. N. Euwema, D. J. Stukel, and T. C. Collins, in *Computational Methods in Band Theory*, edited by P. M. Marcus, J. F. Janak, and A. R. William (Plenum, New York, 1971).

[3] R. N. Euwema, T. C. Collins, D. G. Shankland, and J. S. DeWitt, Phys. Rev. 162, 710 (1967).

[4] R. N. Euwema and D. J. Stukel, Phys. Rev. B 1, 462 (1970).

[5] D. J. Stukel, R. N. Euwema, T. C. Collins, F. Herman, and R. L. Kortum, Phys. Rev. 179, 740 (1969).

[6] See the review of M. L. Cohen and V. Heine, in *Solid State Physics*, edited by H. Ehrenreich, F. Seitz, and D. Turnbull (Academic, New York, 1970), p. 37; and M. L. Cohen, in *II-VI Semiconducting Compounds*, edited by D. G. Thomas (Benjamin, New York, 1967), p. 462.

[7] T. K. Bergstresser and M. L. Cohen, Phys. Rev. 164, 1069 (1967).

[8] J. R. Chelikowsky and M. L. Cohen, Phys. Rev. B 10, 5095 (1970); 14, 556 (1976).

[9] A. Zunger and A. J. Freeman, Phys. Rev. B 15, 5049 (1977).

[10] A. Zunger and A. J. Freeman, Phys. Rev. B 17, 2030 (1978).

[11] L. Ley, R. A. Pollak, F. R. McFeely, S. P. Kowalczyk, and D. A. Shirley, Phys. Rev. B 9, 600 (1974).

[12] D. E. Eastman, W. D. Grobman, J. L. Freeouf, and M. Erbudak, Phys. Rev. B 9, 3473 (1974).

[13] N. B. Kindig and W. E. Spicer, Phys. Rev. 138, A561 (1965).

[14] C. J. Vesely and D. W. Langer, Phys. Rev. B 4, 451 (1971).

[15] A. Zunger and A. J. Freeman, Phys. Rev. B 15, 4716 (1977).

[16] A. Zunger and A. J. Freeman, Int. J. Quantum Chem. Suppl. 10, 383 (1976).

[17] S. R. Das, P. Nath, A. Banerjee and K. L. Chopra, Solid State Commun. 21, 49 (1977).

[18]R. F. Leheny and J. Shah, Phys. Rev. Lett. **37**, 871 (1976).

[19]R. F. Leheny and J. Shah, Phys. Rev. Lett. **38**, 511 (1977).

[20]J. C. Slater, Phys. Rev. **81**, 385 (1951).

[21]R. C. Chaney, E. E. Lafon, and C. C. Lin, Phys. Rev. B **4**, 2734 (1971); D. M. Drost and J. M. Fry, *ibid*. **5**, 684 (1972); E. E. Lafon, R. C. Chaney, and C. C. Lin in *Computional Methods in Band Theory*, edited by P. M. Marcus, J. F. Janak, and A. R. Williams (Plenum, New York, 1971), p. 784.

[22]J. Callaway and J. L. Fry, in Ref. 2, p. 512.

[23]A. Zunger and A. J. Freeman, Phys. Rev. B **16**, 2901 (1977).

[24]Note that the resulting fractional charges do not necessarily bear a relationship to the actual *dynamic* effective charges inferred from e.g., infrared absorption. Instead, these *statically* determined charges reflect the optimal ionic configurations that best span the variationally determined crystal density, within a superposition model.

[25]T. A. Asada, A. Zunger, and A. J. Freeman (unpublished results).

[26]The multicenter Gaussian projection scheme seems suitable for the self-consistent studies of localized impurities, in which the sharp features of $\Delta\rho\,(\vec{r})$ associated with the screening charge gives rise to a slowly convergent Fourier representation. For more homopolar covalent crystals or moderately ionic system, we find the plane-wave expansion to be substantially more efficient.

[27]The updated charge density is determined from the densities of the two previous iterations using a damping technique with a mixing coefficient of 0.3 for the first four iterations and 0.8 for the subsequent iterations.

[28]To obtain a bound S-$3d$ solution, we place the atom in an external potential well of radius 10 a.u. and depth of −1 a.u., in addition to the regular LDF atomic potential. This does not change the radial shape of the occupied orbitals but serves to contract the otherwise diffuse $3d$ state.

[29]W. Kohn and J. J. Sham, Phys. Rev. **140**, 1133 (1965).

[30]K. S. Singwi, A. Sjölander, P. M. Tosi, and R. J. Land, Phys. Rev. B **1**, 1044 (1970).

[31]J. C. Slater, *Symmetry and Energy Bands in Crystals* (Dover, New York, 1972), p. 339.

[32]Reference 31, p. 342; and R. W. G. Wyckoff, *Crystal Structure* (John Wiley, New York, 1963), p. 110.

[33]P. Cerny, Casopis Mineral. Geol. **2**, 13 (1957).

[34]F. G. Smith, Am. Mineral. **40**, 649 (1955).

[35]F. Herman, R. L. Korum, C. D. Kuglin, and J. L. Shay, in *II-VI Semiconducting Compounds*, edited by D. G. Thomas (Benjamin, New York, 1967), p. 503.

[36]J. E. Simmons, C. C. Lin, D. F. Fouquet, E. E. Lafon, and R. C. Chaney, J. Phys. C **8** 1549 (1975).

[37]Obtained from self-consistent atomic calculations using the same exchange functional as that employed for the band calculations.

[38]C. Sugiura, Y. Hayasi, H. Konuma, and S. Kiyono, J. Phys. Soc. Jpn. **31**, 1784 (1971).

[39]C. Sugiura, Y. Gohshi, and I. Suzuki, Phys. Rev. B **10**, 338, (1974).

[40]G. Lehman and M. Taut, Phys. Status Solidi **54**, 469 (1971); O. Jepsen and O. K. Andersen, Solid State Commun. **9**, 1963 (1971).

[41]T. Sagawa, R. Kato, S. Sato, M. Watanabe, I. Ishii, I. Nagakura, S. Kono, and S. Suzuki, J. Electron. Spectrosc. Related Phenom. **5**, 551 (1974).

[42]J. L. Birman, Phys. Rev. **115**, 1493 (1959).

[43]M. Cardona, M. Weinstein, and G. A. Wolff, Phys. Rev. **140**, 633 (1965).

[44]R. Szargan and A. Meisel, Wiss. Z. Karl Marx Univ. Leipzig, Math Naturwiss **20**, 41 (1971).

[45]W. C. Walker and J. Oszntowski, J. Phys. Chem. Solids **25**, 778 (1964).

[46]A. Zunger and A. J. Freeman, Phys. Lett. A **60**, 456 (1977).

[47]A. B. Kunz, Phys. Rev. B **12**, 5890 (1975).

[48]C. E. Moore, *Atomic Energy Levels*, U. S. Dept. of Commerce, Natl. Bur. Stds. Circ. No. 1 (U.S. GPO, Washington, D. C., 1971), p. 467.

[49]There is some indirect evidence for coupling of the $4d$ band to the itinerant band states; the plasmon transition corresponding to the Cd-$5s$ and S-$3p$ valence electrons, observed by electron energy loss (Refs. 50 and 51), occur at energies that are substantially higher than the calculated free-electron plasma transition (12.9 eV), indicating a strong oscillator strength coupling of the Cd-$4d$ states to the itinerant bands as well as a non-negligible contribution of these d electrons to the static dieelectric screening in the material.

[50]R. L. Hengehold and F. L. Pedrotti, Phys. Rev. B **6**, 2262 (1972).

[51]T. Tomoda and M. H. Mannami, J. Phys. Soc. Jpn. **27**, 1204 (1964).

[52]R. K. Swank, Phys. Rev. **153**, 844 (1967). We use the expression $I_{CB} = \varphi - (\Delta\varphi_s - eV_D) = -4.86$ eV and $I_{VB} \approx \Phi + (\Delta\varphi_s - eV_D) = -7.41$ eV, where I_{CB} and I_{VB} are the positions of the conduction- and valence-band edges, respectively, and the rest of the symbols are defined by Swank.

[53]F. Herman and J. P. Van Dyke, Phys. Rev. Lett. **21**, 1575 (1968).

[54]R. Zallen and W. Paul, Phys. Rev. **155**, 703 (1967).

[55]H. Ehrenreich, Phys. Rev. **120**, 1951 (1960).

[56]W. Paul, J. Appl. Phys. **32**, 2080 (1961).

[57]We have recently developed a fully relativistic version of the local-density band method described in this paper (Ref. 58) and hope to apply it to the study of cubic CdS in the future.

[58]J. -P. Desclaux, A. J. Freeman, and A. Zunger (unpublished).